IEEE Access
Multidisciplinary | Rapid Review | Open Access Journal

Received December 12, 2018, accepted December 31, 2018, date of publication January 7, 2019, date of current version January 29, 2019.

Digital Object Identifier 10.1109/ACCESS.2019.2891241

Analysis of Smart Inverter's Impact on the Distribution Network Operation

TAHA SELIM USTUN[1,2], (Member, IEEE), AND YUKI AOTO[1]
[1]Fukushima Renewable Energy Institute, National Institute of Advanced Industrial Science and Technology, Koriyama 963-0298, Japan
[2]Department of Energy and Environment, Research Institute of Energy Frontier, Tsukuba 305-8560, Japan

Corresponding author: Yuki Aoto (y.aoto@aist.go.jp)

This work was supported in part by the KEIDANREN (Japan Business Federation) Promotion of Environmental Protection Foundation's Research Grant-2018.

ABSTRACT More photovoltaics are deployed at distribution networks and these noticeably cause voltage fluctuations in the distribution system. Use of smart inverters (SIs) is investigated as they enhance grid stability with voltage and frequency support. However, these potentially beneficial operating modes of SIs and their impact on the power system operation are not well-known. Conventional simulation packages do not have the tools to run simulations with these inverters. In order to fill this gap and investigate these points, a brand-new simulation platform called Solar Resource Application Platform for Grid Simulation (Sora-Grid) is being developed. In this paper, Sora-Grid's additional capabilities and its unique approach to integrating SIs into the power flow calculations are presented. Some simulation works have been undertaken to show its operation. Furthermore, the results give an insight into understanding the behaviors of SIs and how they impact the distribution grid operation. A typical distribution network with several residential houses is modeled, and the impact of changing operating conditions and active power output on the system voltage is investigated. Finally, a mathematical model is developed to optimize the SI capacity. The optimum point ensures that maximum solar energy is captured, while fair operation is maintained.

INDEX TERMS Smart inverters, distributed control, distribution grid dynamics, power system modeling, active distribution networks, optimal sizing of smart inverters.

I. INTRODUCTION

Widespread use of Distributed Energy Resources (DERs) creates novel problems in grid operation and control [1]. Environmentalists and some politicians are exploring new ways of deploying more DER based generators, and this requires engineers and system operators to bootstrap new techniques and operation schemes in the traditional electrical network [2], [3]. The intermittency of renewable energy based DERs create supply security issues. Furthermore, inverters are decreasing the overall inertia of the power system causing stability issues such as voltage or frequency. In order to reap the benefits of clean energy while keeping their impact at a low scale, inverters need to provide auxiliary support to grid operation, in the same fashion synchronous generators do. Such devices are called smart inverters (SIs), or inverters with advanced capabilities, and can provide voltage and frequency support [4].

Power companies are known to be notoriously in favor of status quo and refrain from making large-scale changes in their infrastructure. Considering the capabilities of SIs and their potential impact on the system, this lack of motivation is understandable. It is important to run extensive tests with this equipment under varying conditions to study and learn their behavior in different conditions [5]. Unlike bulk generation power plants or control devices such as flexible AC Transmission Systems (FACTS) [6], DER based generators can be placed in almost everywhere. This increases the number of scenarios and cases that should be tested before actual deployment. This can be tackled with software-based simulation platforms, as in this paper, or with hardware in-the-loop studies that emulate a real-life operation scenario and require lots of engineering man-hours [7]. Smart inverters are new in the power system arena and most of the well-established simulation package programs do not have them in their libraries. Those who have implemented them, such as OpenDSS, can support only a few functionalities and not the ones related to frequency control. With the recent popularity, this is expected to change but there is a finite learning curve for the industry to

catch up [8]. Feeling this need and seeing this knowledge gap, a unique simulation platform called Solar Resource Application Platform for Grid Simulation (SoRA-Grid) which inherently models SIs and has the ability to run frequency related functionalities. The capabilities of this software are explained in the coming sections while the simulation results presented in this paper are all obtained from it.

Due to their capabilities, SIs are very popular in research domain. There are works focusing on comparing their operation modes and their effectiveness [9], designing new control modes [10], and their integration with droop functionality to mitigate intermittency of solar generation [11]. Other works focus on their performances in different topologies such as in Hawaii [12], California [13], Japan [14], [15], Costa Rica [16] and Taiwan [17]. There are also works that look at coordinating several SIs for maximum system stability as in [18]. However, most of these studies consider large scale SIs that are connected to the high voltage networks. Voltage fluctuation becomes a big problem in distribution networks, due to cables and high resistances, when there is local generation. Therefore, it is important to study their operation in low-voltage systems that are more likely to have over-voltage issues.

Furthermore, all of these works focus on the immediate impact of SIs on voltage regulation or frequency control. There is need for a research that looks at the long-term of SIs with their functionalities, how they increase the locally generated power, and the revenue. It is important to understand the nature in which SIs impact the amount of captured renewable energy over a period of time and how the voltage-limitation is mitigated so that renewable energy capping is avoided. These two phenomena should be understood well to find the optimum point between having a very expensive SI with a high capacity and a small SI that generates less energy but costs much less.

Following from above, in order to measure the advantages and disadvantages of introduction of SIs to power systems, a thorough investigation is required. Given the differences between distribution networks utilized all around the world, different localities may have different experiences [19]. Japan has made a strategic move from nuclear-dominant power generation mix to a more evenly distributed mix where renewables are envisioned to play a bigger role [20]. Due to historical reasons, power networks in Japan tend to be run stand-alone with very little power exchange. This has programmed power companies to be self-sufficient more than anything else, a reality Japan has to adjust to as well. With an aim to observe the benefits of SIs in distribution systems and the challenges they bring along; a typical residential network has been modeled. Simulations are run with different operating modes of SIs. Their impacts on grid stability and meeting voltage/frequency limitations due to grid code are examined.

The rest of the paper is organized as follows: Section II gives an overview of SIs and their different operating modes. Section III outlines the operating principles of SoRA-Grid simulation platform while Section IV details the typical distribution network utilized in these simulation studies. Section V shows power output and voltage profile when SIs are operating in different modes. Section VI discusses the impact of these results on grid planning and deployment of SIs in residential distribution networks where house-owners are directly impacted by the operation of the system.

II. OVERVIEW OF SMART INVERTERS AND THEIR CAPABILITIES

SI can be defined as inverters with advanced control functions that can be used to help the grid operation such as voltage and frequency support [4]. These devices have the ability to operate in all four quadrants of P-Q plane, and can source and sink P as well as Q, independent from each other. SIs control their power output with respect to local voltage and frequency measurements, thus providing support to the grid.

To decrease the burden on inverter-interfaced generators on the power network, SIs with advanced capabilities are being deployed. These capabilities are not the same across all countries and jurisdictions; and many regions do not have a defined certification procedure to validate the functionality of these devices. As a result, DER system vendors create different versions of the software to be compliant with regional requirements. This adds cost and complexity to the design and certification processes. It also generates disparate testing methods and there is no common set of parameters that can be communicated to the DERs. If a single procedure was created that accounted for all the jurisdictional variations (e.g., a superset of the grid code discrepancies), a single document and procedure could validate all grid code requirements [5].

Initially, IEC/TR 61850-90-7 [4] has defined a list of standardized interoperability functions for DERs. As shown in Table 1, these functions are grouped under nine modes. First seven groups focus on power-related functions that are expected from power converters with advanced capabilities. These functions aim at supporting grid by supplying reactive power (VAR), reactive current or managing real power and supporting frequency. It is documented in the literature that these capabilities will decrease the burden of solar based DERs on the distribution grid, both financially and from operations point of view [21].

As far as Var support is concerned, IEC 61850-90-7 have defined four types of var base when applying %Q to calculate the final output:

- VV1 - Available var output with no impact on watts
- VV2 - Maximum var support based on Wmax
- VV3 – Static Mode with fixed Q output
- VV4 – No Q support

VV1 means that available VAR support will be provided with no impact on watts. The amount of Q that should be exchanged, i.e. injected or absorbed depending on the situation, and the corresponding voltage levels are defined as shown in Figure 1, below. When the voltage is below 97% of its rated value, 50 % of available vars should be injected to

TABLE 1. Smart inverter capabilities listed in IEC61850-90-7.

Modes	Functions
Immediate Control	INV1: grid connect/disconnect
	INV2: adjust max. generation level up/down
	INV3: adjust power factor
	INV4: request active power
	INV5: Pricing signal (charge/disch.)
Volt-Var Management	VV1: Available Var support, no P impact
	VV2: Max. Var support based on Wmax
	VV3: Static Power Converter
	VV4: Passive Mode (No Var support)
Frequency Related	FW21: High freq. reduces P
	FW22: Limiting generation with f
Dynamic Reactive Current Support	TV31: Support during abnormally high or low voltage
Low-high voltage ride-through	"Must disconnect" (MD) "Must remain connected" (MRC)
Watt triggered	WP41: Watt power factor
	WP42: Alternative watt power factor
Volt-watt management	VW51: Volt-Watt management (generation)
	VW52: Volt-Watt management (charging)
Non-power parameters	TMP: temperature
	PS: pricing signal
Setting and Reporting	DS91: Modify DER settings (power conv.)
	DS92: Log alarms and events
	DS93: Selecting status points
	DS94: Time synchronization requirements

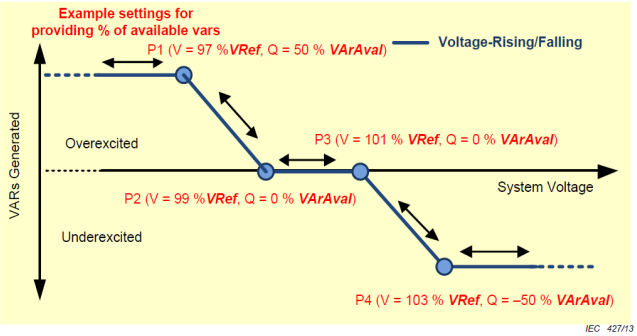

FIGURE 1. VV11 var support mode control curve without hysteresis.

into the system, thus increasing the voltage. When the voltage is between 97 and 99 % of its rated value, Q support follows a linear relationship. For voltage values between 99 and 101 %, the system is stable enough and no support is required. If the voltage exceeds 101% of its nominal value, then SI starts absorbing vars from the system and increases the amount with voltage value until it saturates at 103 %.

Maximum var support based on Wmax follows a similar idea. However, when there is a voltage dip the amount of exported Q is calculated as a percentage of maximum watts the inverter can generate. This ensure that var support provided by an SI is proportional to its ability to generate real power. All the other modes such as frequency-watt (FW21) or voltage-watt (VW51) follow patterns similar to Figure 1, as defined by the standard. More information regarding these modes and their characteristic curves can be found in IEC 61850-90-7 [4].

One of the biggest strengths of SI is the ability to operate in all four quadrants of the P-Q plane. In this fashion, it can be set to operate at a fixed power factor, instructed to change its VAR output according to voltage variation on the point of common coupling or cap its active power generation in conjunction with the allowable voltage levels set forth in the local grid code.

III. SIZING OF SMART INVERTERS FOR FAIR OPERATION

It is possible to model mathematically, the maximum size of a SI in a simple distribution network as shown in Figure 2.

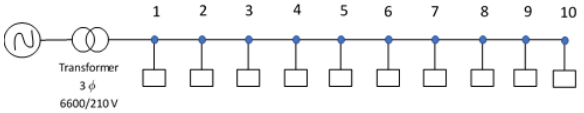

FIGURE 2. A simple distribution network.

In this system, the voltage that should be set to V_{limit} (allowed maximum) is V_n (the last, n^{th} node in the system), as it is the most vulnerable. If that is sustained, the other nodes will always be lower. Assume that all SIs are the same and they generate same P and Q. In this case, they will cause the same voltage increase at each node, due to:

$$(V_{increase} = I_{output} + Z_{line}) \tag{1}$$

Following the typical linear structure of the network in Figure 27, voltage rise at a given node i can be written as:

$$Increase_{node\ i} = V_{increase} * ((n+1) - i) \tag{2}$$

where n is the number of nodes in the system, e.g. 10 for this case. The resultant voltage at a given node is equal to $V_{nominal}$ plus the sum of increases until that node:

$$V_{resultant\ i} = V_{nominal} + V_{increase} * \sum_{1}^{i}(n+1) - i \tag{3}$$

Since the highest increase is at node n, it can be expressed as;

$$V_{nominal} + \left(\frac{n \times (n+1)}{2}\right) * V_{increase} = V_{limit} \tag{4}$$

Grid codes express V_{limit} as a percentage of $V_{nominal}$

$$V_{limit} = (100 + g)\% \text{ of } V_{nominal} \tag{5}$$

where g is the percentage increase allowed by the grid code. Rearranging 4 and 5,

$$V_{increase} = \frac{g \times V_{nominal}}{\left(\frac{n \times (n+1)}{2}\right) \times 100} \tag{6}$$

On the other hand, the voltage increase is caused by the power injected by the SI to the system. In an AC system, this is expressed as:

$$V_{increase} = \frac{RP + XQ}{\hat{V}_s} + j\frac{XP + RQ}{\hat{V}_s} \tag{7}$$

where V_s is the sending end voltage phasor. If the angle between V_s and V_r, i.e. the receiving end voltage phasor, is too small (7) can be simplified as:

$$V_{increase} = \frac{RP + XQ}{\hat{V}_s} \tag{8}$$

Normally, sending end angle is assumed to be zero to convert the phasor of Vs to a scalar. However, in this case, there are several sending ends and a single receiving end, feeder. Same can be done for receiving end voltage, V_r, and the voltage at a given node, i, can be expressed as

$$V_i = V_r + (RP + XQ) \times \sum_{j=1}^{i} \frac{1}{\hat{V}_j} \tag{9}$$

where the highest voltage value is observed at node n, *i.e.* when $i = n$. Equating the voltage rise portion, addition to V_r, with (6), give the relationship between P, Q provided by an SI and the voltage rise induce:

$$\frac{g \times V_{nominal}}{\left(\frac{n\times(n+1)}{2}\right) \times 100} = (RP + XQ) \times \sum_{j=1}^{n} \frac{1}{\hat{V}_j} \tag{10}$$

where n is the number of nodes, g is the percentage of allowed voltage rise in the system allowed by the grid code, R and X line are reactance and resistance, respectively, while P and Q are real and reactive power outputs of SI. Although it is possible to rearrange this equation with Z, impedance and S, apparent power, parameters; it is not possible to simplify it to an equation that can be solved in a trivial manner. Phasors of each nodes along the way, both their magnitudes and angles, should be taken into account. More importantly, in Volt-var mode, e.g. Figure 1, var output is a function of voltage, $Q(V)$, and this makes iterations more difficult.

Therefore, using a simulation platform that works out these values through power flow iterations is much easier. It is possible to set P and Q values, by setting power factor, in which case a fixed relationship between them will be established. Once the equation is solved through iterations, the maximum permissible capacity, S, of a SI in the system can be worked out from

$$S^2 = P^2 + Q^2 \tag{11}$$

IV. A NOVEL SIMULATION PLATFORM FOR SMART INVERTERS

As explained in the previous section, planning and sizing of SI require a tool that can model their impact on the voltage rise with respect to their real and reactive power outputs. To fill this gap a power system simulation tool, SoRA-Grid, is specifically developed to accommodate SI in power networks. The motivation is to investigate impact of Photovoltaic (PV) penetration in distribution networks under varying solar radiation, loading or network conditions. Depending on the focus being short or long-term impact, the studies can be run for a few minutes or a few days [8].

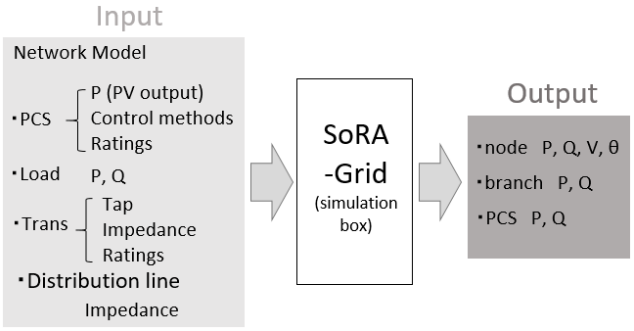

FIGURE 3. SoRA-grid operation.

SoRA-Grid is developed in MATLAB, uses Simulink components to model the network while simulations are run in MATLAB's console. Inputs given and results of power calculations into by CSV files. As conceptualized in Figure 3 below, PV generation patterns for each SI, power demand profile (P, Q) for each load can be inputted with resolutions down to a minute. Different operation modes (Volt-Var Control, and Volt-Watt Control and Power Factor Control etc.) can be set for different SI. It is also possible to set operation of transformer taps and their schedules.

Since SI is a component that actively contributes to power exchange in the system, it disrupts natural flow of power flow iterations. SoRA-Grid implements the following iteration approach:

1. *Solve the system with normal Power Flow Iterations*
2. *Solve for V, P and Q values for all nodes*
3. *For nodes where a Transformer, SI or a battery is connected, use these initial V, P, Q values to detect its reaction (e.g. a SI may inject P, or a transformer may change its tap etc.)*
4. *With new values of nodes due to changes in 3, re-run step 1 and 2.*
5. *Repeat above process until the power flow calculations accommodate all SI reactions and a steady-state is reached.*

It goes without saying that it is possible to run these SIs as traditional inverters and such cases can be used as benchmark cases to compare with other scenarios where advanced inverter capabilities are activated.

V. DISTRIBUTION NETWORK MODELING

In order to investigate impacts of novel capabilities incorporated into SIs, extensive studies have been run. The benefits, such as frequency or VAR support, as well as drawbacks, such as excessive voltage rise are examined. To achieve this, a typical distribution network, shown in Figure 4, is modeled. It is a radial network with 12 branches that feed 4 houses each.

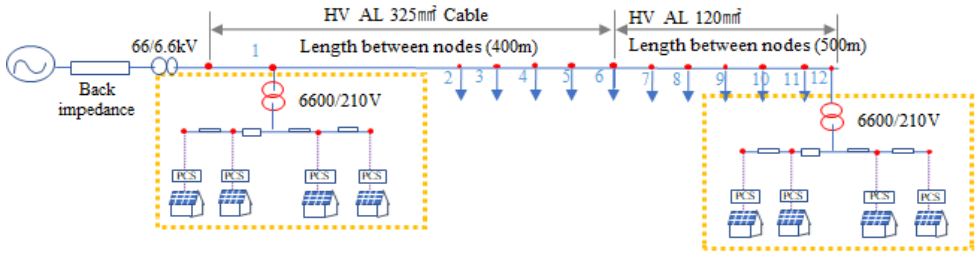

FIGURE 4. Distribution system model for residential area.

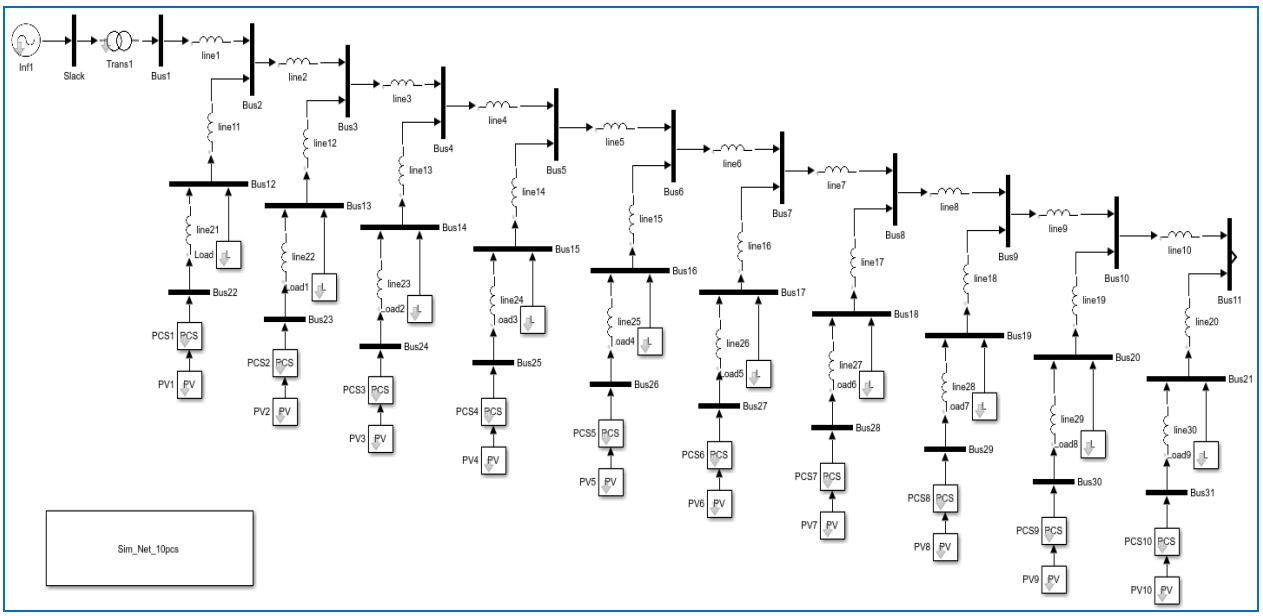

FIGURE 5. System modeling in SoRA-grid (with Matlab/Simulink GUI.

The infinite bus is connected to the network over a 66kV:6.6kV transformer while individual branches further reduce this to 210 V. These distribution networks use center tapped secondary, so that the input voltage to a household is 105 V and no ground connection is needed. The parameters of large step-down transformer (66:6.6 kV) and smaller pole transformers (6.6kV:210V) are given in Table 2.

TABLE 2. Feeder transformer parameters.

	Feeder Transformer	Pole Transformer
Rated capacity [kVA]	600	50
Primary voltage [V]	66000	6600
Secondary Voltage [V]	6600	210
tap voltage [V]	66000	6600
Z [Ω]	3.08 + j21.56	0.005+j0.0082

Line impedances, including the back impedance, are also modeled for each distribution line and drop-line connection. It is a practice to use a larger distribution cable for the first half of the network and a smaller cable on the second half, as the previous one carries the energy for all connections. In this model the length of these cables is 400m and 500 m between two nodes, respectively. In each node, looking downstream, there is a pole transformer followed by another distribution cable, this time a low voltage one. Finally, drop cables are used to connect households to the lines. These line impedances are given in Table 3.

TABLE 3. Line impedances.

Cable Type	Impedance	Length
Back impedance	j1.21[Ω]	N/A
HV AL 325 mm2	0.0945+j0.1103 [Ω/km]	400 m
HV AL 120 mm2	0.4000+j0.3480 [Ω/km]	500 m
LV AL 120 mm2	0.3550+j0.2680 [Ω/km]	50 m
LV 3.2 mm2 (drop)	2.005+j0.0940 [Ω/km]	20 m

The final drop line connection represents connection to three individual households each of which has PV modules, a SI and a load, as shown in Figure 5. Considering the typical

size of houses, and their roofs, a 3 kW PV system is modeled. Houses are assumed to have same load profiles, P and Q, which are modeled based on a local utility's measurements as shown in Figure 6.

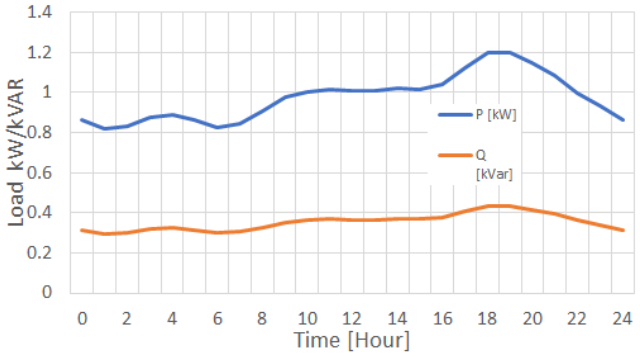

FIGURE 6. Load Profile of an individual household.

Each of the SIs has the capability to run in one of the following modes:

- Q control Mode, where the reactive power output of the inverter is set, real power, P, can assume any value as long as it is within the capacity of the SI
- Power factor mode, where the power factor is set to a desired value
- Volt-Var mode, where the reactive power output of the inverter is controlled with respect to the system voltage.

Several simulations have been run where different SI are running in different modes. Furthermore, solar curtailment to limit voltage rise in the distribution system has been implemented. In this fashion, these cases can be compared with baseline case where no such limitation is imposed. Figure 7 shows the real power output of each node (represents lumped behavior of 4 SIs) where no voltage limitation is imposed. Only one curve is visible as all nodes have the same real power output and a reactive power output of zero. Figure 8 shows the voltage values for each node, and it is evident that voltage levels at some downstream nodes exceed the maximum permissible value set by the grid code.

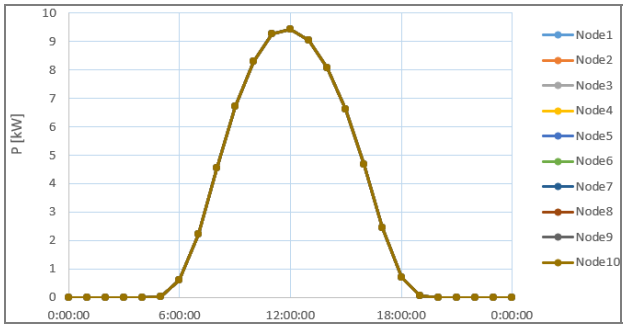

FIGURE 7. Real power output without voltage limitation.

The basic measure taken to avoid this phenomenon is to limit real power output, P, when the node voltage reaches the maximum permissible value as per the grid code. This feature is also implemented in all conventional inverters. In this case, as shown in Figure 9, since the voltage rise is directly related to the relative location of the inverter with respect to grid connection, an unfair situation appears. Inverters that are further away from the feeder connection, i.e. downstream, need to limit their output much sooner, as shown in Figure 10.

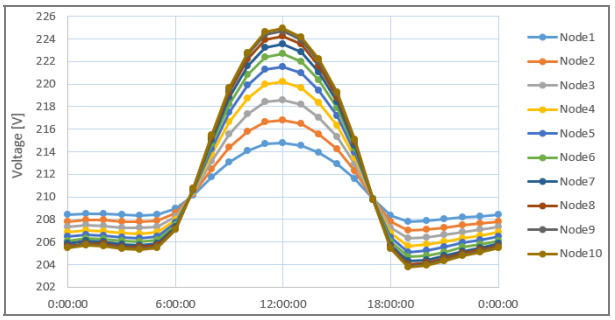

FIGURE 8. Node voltages without voltage limitation.

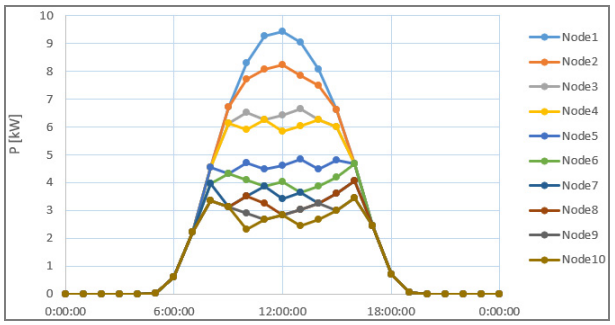

FIGURE 9. Real power output with voltage limitation.

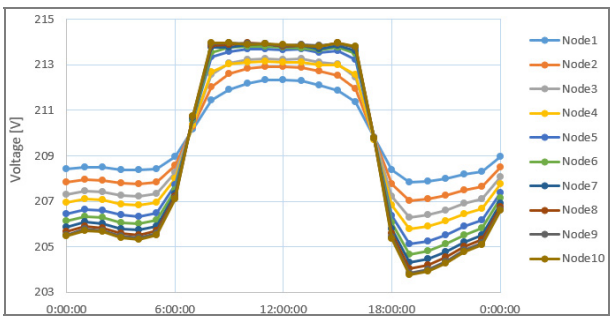

FIGURE 10. Node voltages with voltage limitation.

This creates a difficult problem for policy-makers and household owners. Houses located in the same distribution network enjoy different levels of energy export capacity, merely depending on their proximity to the feeder connection point. In other words, for the same amount of investment, house owners will get different return on investment. This creates a big hurdle in convincing public into purchasing PV modules with SIs, unless a fair solution is found.

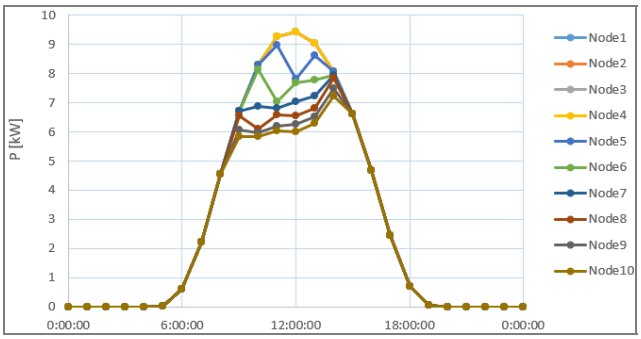

FIGURE 11. Real power output with Volt-Var control.

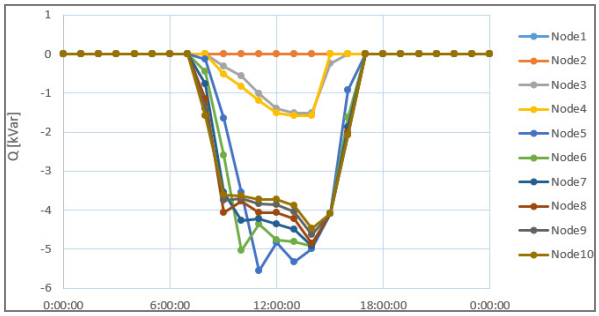

FIGURE 12. Reactive power output with Volt-Var control.

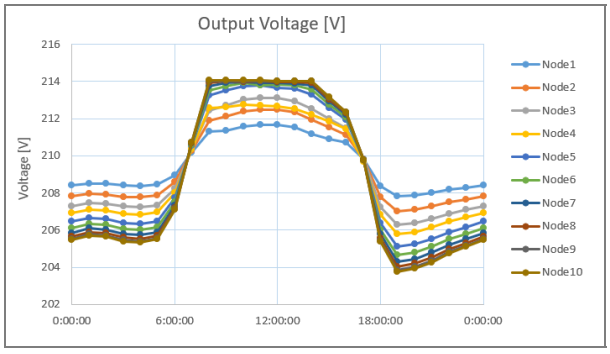

FIGURE 13. Node voltages with Volt-Var control.

One of the ways to tackle this issue is to run SIs in Volt-Var mode where their VAR output changes with node voltage, see [4] for details. Rising node voltage triggers SIs to absorb more VARs to help reduce the local voltage. As shown in Figure 11, in this mode, every node contributes to reducing the local voltage rise and curtailment amount is reduced, though not eliminated. Still, a fair operation is not achieved, due to the fact that Volt-Var control is based on the local node voltages. Therefore, downstream inverters dedicate their capacity to VAR absorption, much sooner than their upstream counterparts. For an unlimited capacity, this may not prove to be problematic. However, for limited capacities, this means downstream inverters saturate their capacity with VAR absorption and cannot output same amount of real power. In such situations, extra capacity for downstream inverters must be subsidized by government or other agencies, so that with the extra capacity, they can output the same real power. Another approach is to compensate downstream inverters for their Q support, instead of only making payments for amount of exported P.

An alternative approach suggests that all inverters should use same amount of their capacity for Q support in the grid. In such a case, the burden of voltage control will be equally distributed among inverters. PF mode of Smart Inverters can be utilized to set a fixed amount of Q output (or absorption) for a certain amount of P generation. In the test scenario, when all the inverters are set to run in 0.85 power factor mode, a fair operation is achieved as shown in Figures 14 and 15. Simulations run with different PF setpoints yielded different results. Choosing appropriate PF setpoint for systems with different inverter sizes, load profiles and solar radiation (i.e. PV output) is an open research field and a future work item. Another parameter that can be changed is the capacity of the SI. In this fashion, a fair operation can be achieved with much smaller investment on the equipment.

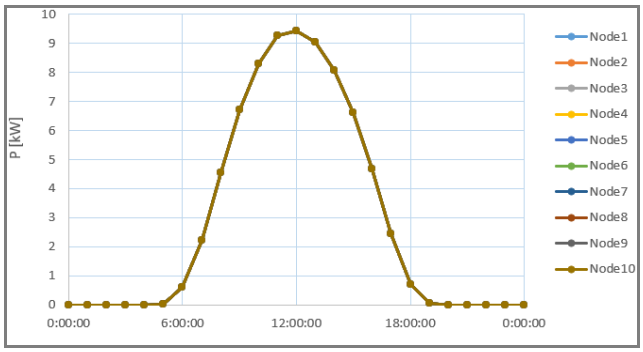

FIGURE 14. Real power output with PF = 0.85.

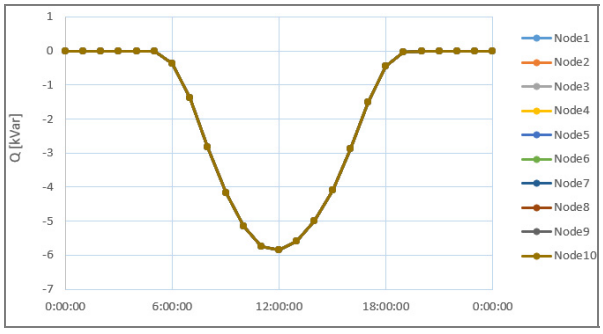

FIGURE 15. Reactive power output with PF = 0.85.

Figures 16, 17 and 18 show P, Q and voltage profiles when the capacity of SIs is reduced from 3 kVA to 2 kVA (12 kVA to 8 kVA per node). Unlike the previous case, i.e. capacity = 12 kVA, real power P generation saturates, and Q output follows along. Local voltage profile shows that maximum levels are not reached, even at the peak power generation point. This shows that there is an optimum capacity where the

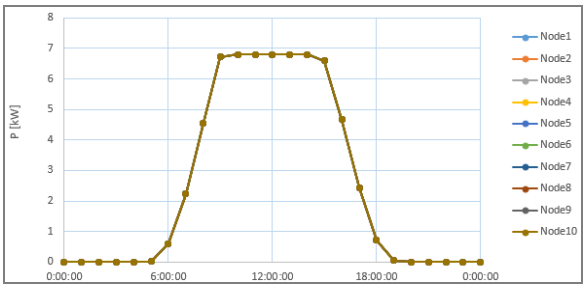

FIGURE 16. Real power output for 8kVA node capacity.

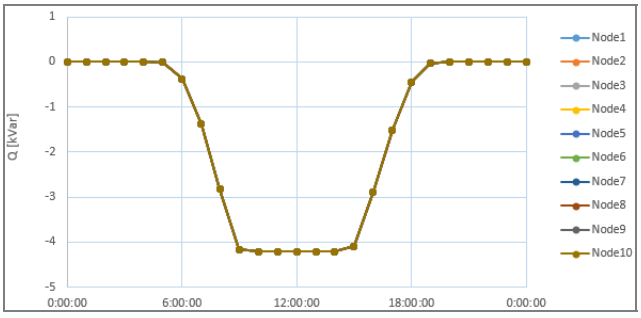

FIGURE 17. Reactive power output for 8kVA node capacity.

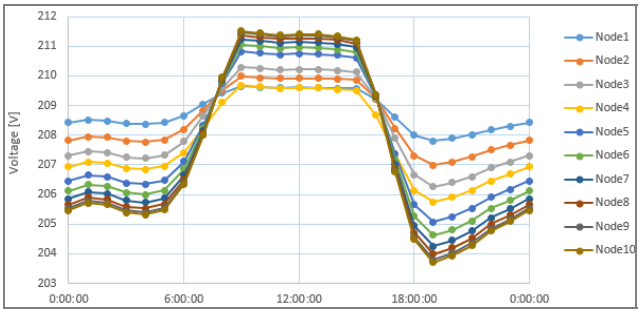

FIGURE 18. Node voltages for 8kVA node capacity.

investment is not as large, voltage rises are more manageable, and a fair operation is achieved. A thorough algorithm that yields the most optimum sizing and/or power factor set point for a given inverter size needs to be investigated.

VI. OPTIMAL SIZING CONSIDERATIONS

Use of SI in PV systems introduces novel research questions such as fair-use of the public electric grid, different pricing schemes to maximize the overall output and to minimize the difference between different households. In this section, a fair operation is assumed where all SIs connected to the same distribution network generate the same amount of energy. Then, the voltage rise in a particular network and the corresponding cap on generation are studied for different SI/PV panel ratios with the motivation of finding the most optimum one.

During these studies, five representative irradiation patterns of Koriyama City are utilized to reflect the impact of real-life variation of available solar power. As compared to static annual or monthly average patterns, this approach has the benefit of quantifying the days where the overloading has an actual impact on the generation. A novel simulation software, SoRA-Grid, developed by FREA is utilized to run power flow studies on a distribution network and over-voltage protection limitations have been enforced. The results are compared in terms of the revenue generated from power injected to the grid, utilization of the installed SI and how much of the available solar energy is harvested by the system.

A. CATEGORIZED WEATHER DATA USED IN SIMULATIONS

Irradiation pattern which is fed to SoRA-Grid is the most important input data since the resultant PV output power is calculated from it. It is more common to use monthly or annual averages of solar radiation patterns. However, such averaging causes loss of resolution and extreme high, as well as low, points where PV generation limitation may occur are not taken into account. Therefore, effective average of solar radiation from PV plant's generation point of view would be lower. While using the measured data of every day for an entire year is the most accurate approach, it is not feasible due to volume of the data that needs to be processed. In order to include the impact of varying radiation in a reasonable fashion a classification approach has been utilized in this research.

Based on two different indices, i.e. Variability Index (VI) and Clear Sky Index (CI), five basic irradiation models have been used to categorize annual data [22]. As shown in (12), VI is the ratio of the length of the measured global horizontal irradiance (GHI) and the length of the clear sky GHI. On the other hand, CI is a metric used to quantify the amount if available solar radiation that reaches the ground and it is shown in (13).

$$\mathrm{VI} = \frac{\sum_{k=1}^{n-1} \sqrt{(\mathrm{GHI}_{k+1} - \mathrm{GHI}_k)^2 + (t_{k+1} - t_k)^2}}{\sum_{k=1}^{n-1} \sqrt{(\mathrm{CHI}_{k+1} - \mathrm{CHI}_k)^2 + (t_{k+1} - t_k)^2}} \tag{12}$$

$$\mathrm{CI} = \frac{\sum_{k=1}^{n-1} \frac{\mathrm{GHI}_{k+1}+\mathrm{GHI}_k}{2} (t_{k+1} - t_k)}{\sum_{k=1}^{n-1} \frac{\mathrm{CHI}_{k+1}+\mathrm{CHI}_k}{2} (t_{k+1} - t_k)} \tag{13}$$

where GHI is Global Horizontal Irradiance and CHI is Clear-sky Horizontal Irradiance, both of which are expressed in [W/m^2] and taken at time tk.

With the help of CI and VI, 5 distinct patterns corresponding to Clear sky, Overcast sky, Moderate variability, Mild variability and High variability are extracted. Table 4 shows

TABLE 4. VI and CI criteria for classification.

Pattern Name	CI	VI
Clear	≧0.5	<2
Overcast	≦0.5	2
Moderate	X	2≦VI<5
Mild	X	5≦VI<10
High	X	>10

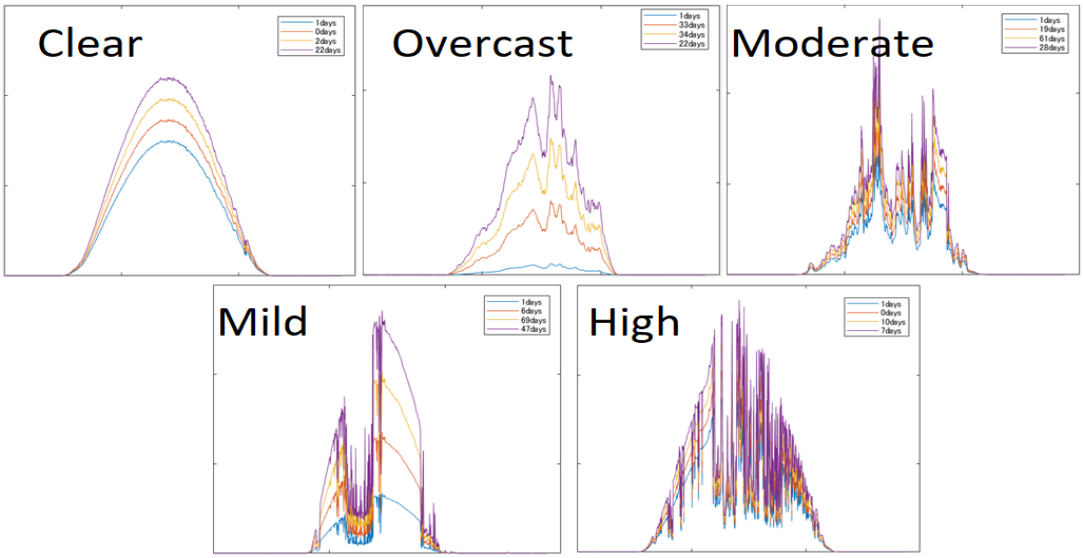

FIGURE 19. Different variability patterns and their annual distributions.

the criteria utilized for these patterns. The data used is the solar irradiation is measured at FREA's facilities. It is the recorded minute-average for an entire year (2017). Normally, PV modules are installed with a tilt angle to maximize the captured solar radiation. Therefore, a module tilt angle of 20° is considered instead of GHI. The results are shown in Fig.19.

After this classification, each pattern is divided into 4 different scales which are equally distributed between maximum and minimum peaks. In this fashion, differed irradiation levels corresponding to same variability pattern are distinguished from each other. Also, number of days in which a particular pattern (and one of its 4 sub-scales) is determined.

Equation (14), shows how the maximum possible PV output is calculated from these irradiation patterns, installed capacity of the PV and a loss factor K. For the ease of calculation, the generation is calculated in 1-hour time steps (instead of a minute).

$$PVout_t = PV_{cap} \times Irrad_t \times K \tag{14}$$

where Irradt is solar irradiation [W/m^2] and PVcap is PV capacity in kWs, and K is an efficiency factor of 0.85 which considers losses due to the inverter, wiring and others causes. Fig.20. shows PV output for each pattern and its sub-scales.

These patterns give valuable information on how clear or how variable months or seasons in a particular location. For example, Table 5 shows the distribution of these patterns among months and seasons. It can be observed that Moderate and Mild are the most frequent patterns in Koriyama city while Clear and High are very rarely observed. Furthermore, as shown in Figure 21, Clear never appears in Winter months, while Summer months are dominated by High variation.

Multiplying PV output values with the number of occurrences in a year gives the maximum available power from

TABLE 5. Frequency of irradiance patterns in Koriyama.

Month	Clear	Overcast	Moderate	Mild	High
Jan	0	7	9	14	1
Feb	1	4	10	9	4
March	1	9	11	5	5
April	2	2	15	10	1
May	8	4	6	10	3
June	0	2	10	6	12
July	4	6	9	7	5
August	0	6	12	8	5
Sept.	1	5	11	8	5
Oct.	1	12	6	11	1
Nov	0	10	7	13	0
Dec.	0	9	6	15	1
Total	18	76	112	116	43

PV systems without any limitation from undersizing of the SI and/or voltage rise in the distribution network. These are reflected on the results with the simulations that are run on SoRA-Grid as explained in the next section.

B. SIMULATION RESULTS

Firstly, the modeled distribution system is run with different SI/PV ratio and the performance is observed. Since this is meant to serve as a base case scenario, no voltage limitation is enforced. This also removes the effect of location on the power output and helps understand its impact on SI output later. SI/PV ratio is varied from 100 % to 20 %. The lower ratio corresponds to the threshold where the SI capacity is only sufficient to feed the local load and there is no extra power that can be exported. All the other ratios correspond to

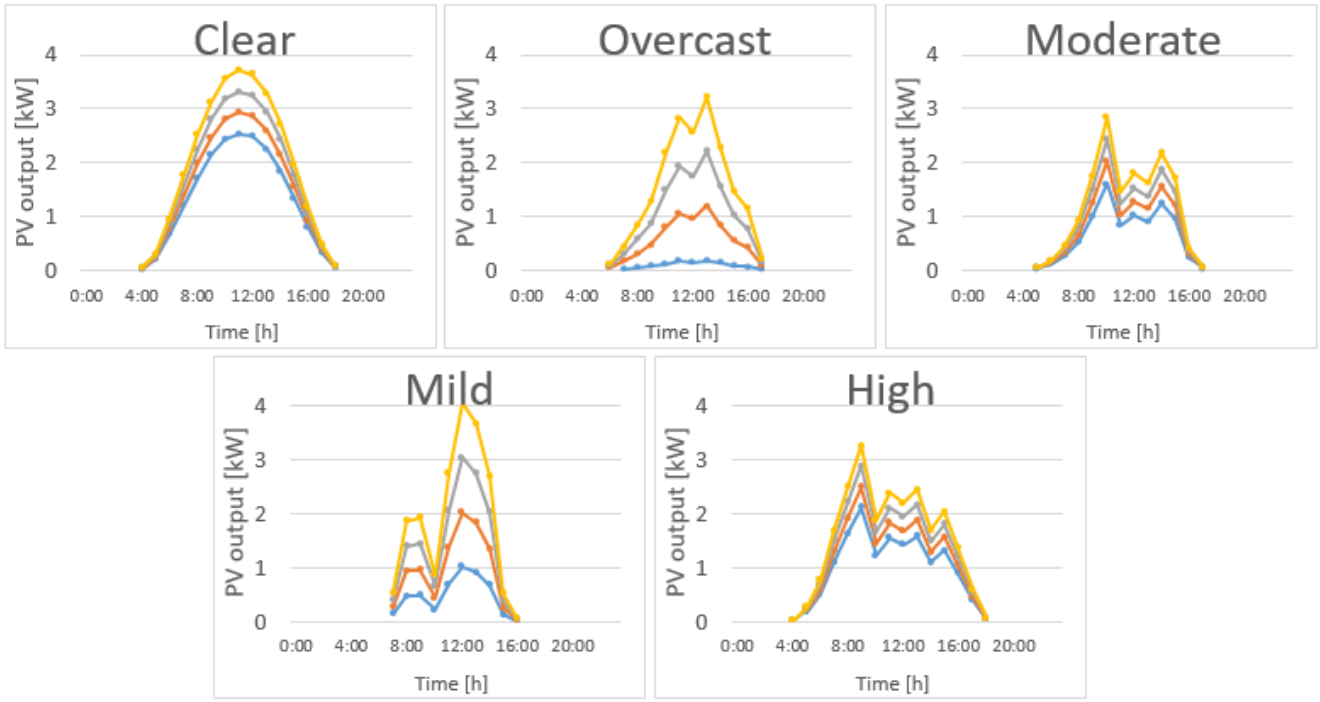

FIGURE 20. PV output for different variability patterns.

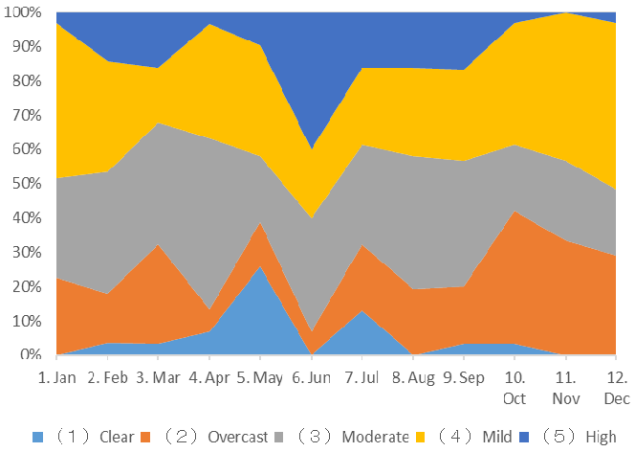

FIGURE 21. Monthly variability conditions vs. % of days.

different amounts of surplus power. Table 6 shows the annual power output and the surplus that is injected to the grid for this base case.

The natural flow of the simulation requires that first upper voltage limitation is enforced as per the national grid code. In Japan, distribution networks are limited to a 202 ± 20 Volts. Therefore, in this step, SoRA-Grid simulates the entire network, and enforces a maximum voltage limit of 222 V on every SI. The total power generation and the surplus amount decrease as Table 7 shows. As the SI/PV ratio decreases, the capacity of SI and its ability to export power become lower. 60 % ratio seems to be the cut-off point since higher ratios experience power caps due to voltage rise, while lower ratios follow the base case.

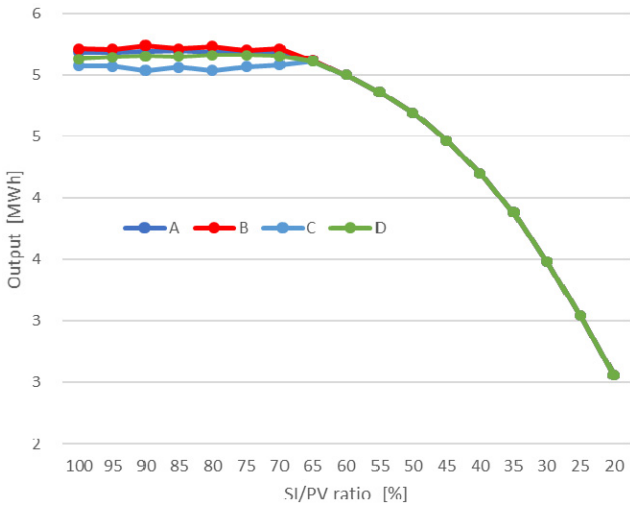

FIGURE 22. Effect of voltage limitation on SI outputs.

As expected, households that are farther away from the feeder connection are affected more and their generation is limited. On the other hand, houses nearer to the feeder enjoy the voltage stability and can export more energy. Figure 22 below shows how houses A, B, C and D have different outputs until the 60 % ratio, after which all households have the same output (and a fair environment is achieved). Similarly, Figure 23 shows the amount of power

TABLE 6. Annual power output and surplus power (no upper voltage limit).

SI/PV ratio	SI capacity [kVA]	Annual Power Output (MWh)	Annual Surplus (MWh)
100	4	780.833	388.318
95	3.8	779.480	386.964
90	3.6	777.198	384.682
85	3.4	772.748	380.232
80	3.2	767.698	375.183
75	3	760.619	368.104
70	2.8	751.362	358.847
65	2.6	737.185	344.669
60	2.4	719.909	327.393
55	2.2	699.827	307.311
50	2	675.424	282.908
45	1.8	643.521	251.005
40	1.6	604.868	212.352
35	1.4	559.017	166.501
30	1.2	501.883	109.368
25	1	438.209	45.704
20	0.8	368.930	0.000

TABLE 7. Annual power output and surplus power (upper voltage limit of 222V enforced).

SI/PV ratio	SI capacity [kVA]	Annual Power Output (MWh)	Annual Surplus (MWh)
100	4	743.422	350.906
95	3.8	743.884	351.368
90	3.6	744.525	352.009
85	3.4	743.752	351.237
80	3.2	744.594	352.078
75	3	743.991	351.476
70	2.8	743.961	351.446
65	2.6	736.644	344.128
60	2.4	719.909	327.393
55	2.2	699.827	307.311
50	2	675.424	282.908
45	1.8	643.521	251.005
40	1.6	604.868	212.352
35	1.4	559.017	166.501
30	1.2	501.883	109.368
25	1	438.209	45.704
20	0.8	368.930	0.000

lost (i.e. power which would, otherwise be harvested) due to voltage limitation.

While selecting a smaller SI/PV ratio seems to be a good solution from these results, it has a negative impact on the ability to harvest the available solar energy. It is true

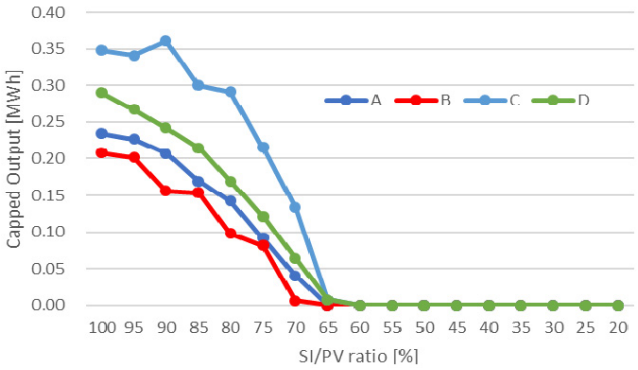

FIGURE 23. Capped power due to voltage limitation per household.

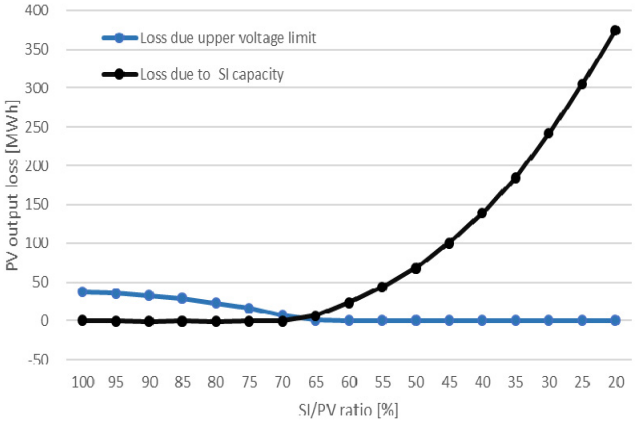

FIGURE 24. Amount of unharvested available energy.

that smaller SI capacity means lower capital costs, however, as Figure 24 shows, the amount of uncaptured available energy becomes very high for lower ratios.

Looking it individual houses, smaller SI capacity brings everybody to a level playing field, which means privileged houses such as A and B will experience larger energy loss (unharvested energy) as shown in Figure 25. 60 % ratio, again, seems to be the threshold, where the losses are even, and the generation is fair.

VII. DISCUSSIONS ON FINDINGS AND THEIR IMPLICATIONS

The obtained results are evaluated based on three different parameters, which are Capacity Factor (CF), Energy Capture Factor (ECF) and payback time.

A. CF AND ECF CALCULATIONS

As the simulation results show, varying SI size has impact on the amount of harvested energy (from the available amount) and the amount of limitation imposed due to voltage rise in the electrical network. Too large SI size is ultimately limited by the voltage rise, while too small SI size captures too little solar energy. The optimum point lies somewhere in between these two extremes. In order to have a structured evaluation,

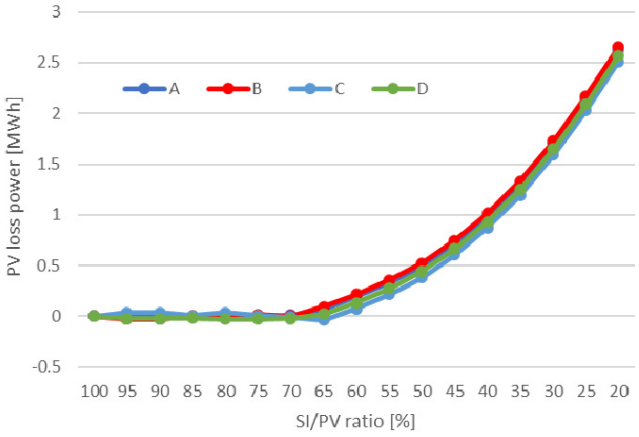

FIGURE 25. Amount of unharvested available energy per household.

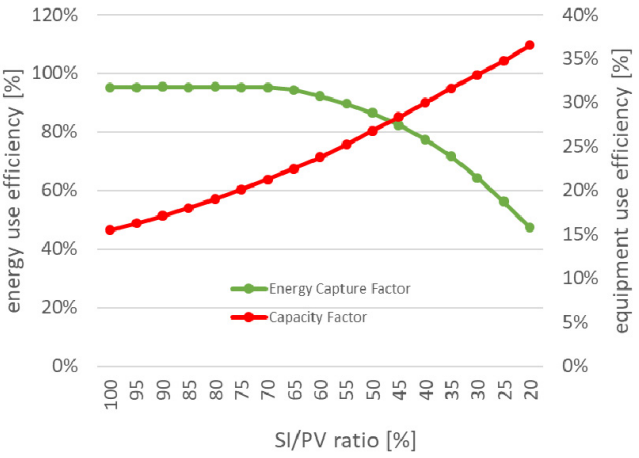

FIGURE 26. CF and ECF values for different SI/PV ratios.

in addition to well-known CF, a new parameter, namely ECF, has been defined. It indicates what percentage of the solar energy harvested by the PV module is captured by the SI. These parameters are given in (15) and (16).

$$CF = \frac{\sum_{d=1}^{365}\sum_{h=0}^{23} SI_{out}}{\sum_{d=1}^{365}\sum_{h=0}^{23} SI_{cap}} \tag{15}$$

$$ECF = \frac{\sum_{d=1}^{365}\sum_{h=0}^{23} SI_{out}}{\sum_{d=1}^{365}\sum_{h=0}^{23} PV_{out}} \tag{16}$$

where SI_{out} is the actual power output of the SI, SI_{cap} is the SI capacity and PV_{out} maximum available power harvested by the PV module. These values are summed over every hour of the day and every day of the year. The results for different SI/PV ratios are plotted in Figure 26.

It is observed that the amount of energy that is captured is almost constant until 70%, after which is has a deep dive. On the other hand, CF increases steadily with smaller SI/PV ratios. The crossover point is located between 50 and 45%.

B. CAPTURED ENERGY vs. INVESTMENT EVALUATIONS

The most important parameter in evaluation is the payback time, i.e. the relationship between the initial investment the revenue generated by the system built with it. The costs are made up of three major components: initial capital cost, annual maintenance costs and SI replacement cost which occurs once in every 10 years [23]. Japan has subsidies in place for renewable energy projects and this is subtracted from the initial capital cost. In Fukushima prefecture, this is 40,000 yen/kW and it has an upper limit of 160,000 yens [24]. To calculate the overall cost of the system, local prices have been gathered as shown in Table 8. The corresponding initial costs are calculated as in equations below.

$$\text{Cost}_{\text{PV}} = \text{Cost}_{\text{sys1kW}} \times \text{PV}_{\text{cap}} \times \text{PV}_{\text{sysrate}} \tag{17}$$

$$\text{Cost}_{\text{SI+Other}} = \text{Cost}_{\text{sys1kW}} \times \text{SI}_{\text{cap}} \times (100 - \text{PV}_{\text{sysrat}}) \tag{18}$$

$$\text{Cost}_{\text{total}} = \text{Cost}_{\text{PV}} + \text{Cost}_{\text{SI+Other}} \tag{19}$$

TABLE 8. Costs of system components.

	Symbol	unit	value
PV capacity	PV_cap	kW	4
SI capacity	SI_cap	kVA	variable
SI/PV ratio	SI_rate	%	20～100 (5%++)
Equipment cost 1kW[25]	Cost_sys_1kW	yen/ kW	364,000
PV's Share in overall cost[25]	PV_sys_rate	%	52
SI's share in overall cost [25]	SI_sys_rate	%	11
Maintenance cost 1kW	Cost_mtn_1kW	yen/kW /year	1,200
SI replacement	Cost_pcs_chg	yen	variable

Based on [23], the annual maintenance cost can be assumed as 1200 yen/kW. It is required to add the SI replacement cost which happens once in a decade. The final annual maintenance cost can be expressed as;

$$\text{Maint}_{\text{Annual}} = 1200 + (\text{Cost}_{\text{sys1kW}} \times \text{SI}_{\text{cap}} \times \text{SI}_{\text{sysrate}})/10 \tag{20}$$

The system has two income streams which are revenue generated by sales to the grid and the avoided costs with local generation, i.e. amount of power which would, otherwise, be purchased from the grid.

Total surplus power is calculated as:

$$Surplus_{nel} = \sum_{d=1}^{365}\sum_{h=0}^{23}\sum_{node=1}^{12} SIsurplus_{node} \tag{21}$$

Annual revenue generated by a house, on average, is:

$$\text{Income}_{\text{year}} = (\text{Surplus}_{\text{net}}/\text{Home}_{\text{num}}) \times \text{Income}_{1\text{kW}} \tag{22}$$

TABLE 9. Parameters used for income calculations.

	Symbol	Unit	Value
Yearly total surplus power by network.	Surplus_net	MWh	-
Number of homes at network.	Home_num	home	144
Hourly SI output at each node.	SI_out_n	MWh	-
Hourly Load at each node	Load_n	MWh	-
Hourly Surplus power at each node.	SI_surplus_n	MWh	-
Yearly total surplus power by 1 house.	Surplus_1home	kWh	-
Yearly income by power selling 1 house.	Income_year	yen	-
Power selling cost by 1kW (for house)	Income_1kw	yen/kW	28
Annual reduction per house	Reduction_house	yen	-
Monthly fixed price	Fee_base	yen	257
Monthly kWh price	Loadsupply_month	kWh	-
Daily load supply electricity per house	Loadsupply_daily	kWh	-
Electricity Price (over 7kWh)	Fee_over	yen/kWh	18.24

The annual bill reduction per house, due to local generation and avoided purchase from the grid, can be worked out as:

$$Reduction_{house} = \sum_{node=1}^{12} (Fee_{base} + \sum_{d=1}^{dmax} Fee_{over} * (Load_{month} - 7kWh) \quad (23)$$

Finally, an overall cashflow calculation has been performed for 40 years where a simple net income equation has been used:

$$\text{Cash\_flow} = -(\text{Cost}_{\text{total}} - \text{Subsidy}) - \text{Maint}_{\text{annual}} + \text{Income}_{\text{year}} + \text{Reduction}_{\text{house}} \quad (24)$$

When the calculations are performed, different payback times have been obtained for different sizes, since larger systems require more investment, but can generate more income due to larger renewable energy generation. The results are plotted in Figure 27 while detailed cashflow data is given in Appendix. It is observed that the figure reaches minimum values between 65 and 50 % ratios. Considering this, 65 % value is the optimum point for this study (with its particular radiation pattern and network parameters), since it has the lowest payback time with the highest SI/PV ratio. This means it will generate more energy than others (i.e. 60, 55 or 50%) once the payback is reached.

VIII. CONCLUSIONS

This paper ventures into studying the impacts of SIs, on the distribution network. Since conventional simulation packages do not have the means to model them, a novel software, Sora-Grid is developed. With the help of Sora-Grid, SI behavior under different operating conditions is examined to see the impact on voltage control, power output and fair operation for all stakeholders. Future work focuses on how to plan optimum SI sizes considering local constraints of voltage rise. Furthermore, in this research all of the SIs are run in the same mode. The optimum mix of SI capabilities run at a certain point in time is also very important. With these advanced capabilities, maximum amount of energy can be harvested while supporting voltage and frequency stability in the system.

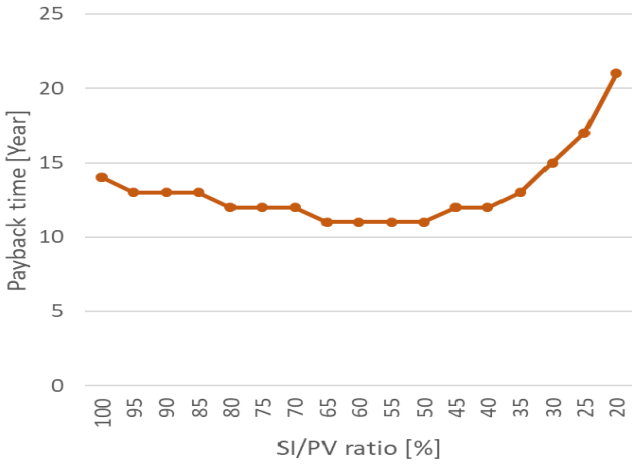

FIGURE 27. Payback time vs. SI/PV ratio.

Addition of SI into distribution networks not only provides auxiliary services but also creates new paradigms which should be taken into account in planning. This work shows the impact of P control (limiting P to prevent voltage rise) on the operation and overall generation. Furthermore, it categorizes solar radiation in a particular location, Koriyama, based on their variability and uses them to investigate their overall impact on the local generation. Combining these two considerations, an optimal SI/PV ratio study has been conducted for a typical distribution network. Results show that too small SI/PV ratios cannot capture major portion of the locally available radiation while too large SI/PV ratios have too much capacity which is not mostly used due to voltage limitations. For this particular study, an overall optimum point is found to be at 65 % where the SI capacity is large enough to capture most of the local solar energy while it does not get effected by the voltage limitations, as its generation does not cause such incidents. These results are valid for the power system modeled (including ratings and parameters) as well as the radiation pattern that belong to Koriyama. For other networks or locations, similar studies should be run as the results may differ. In any case, a similar pattern can be expected while optimum point may vary.

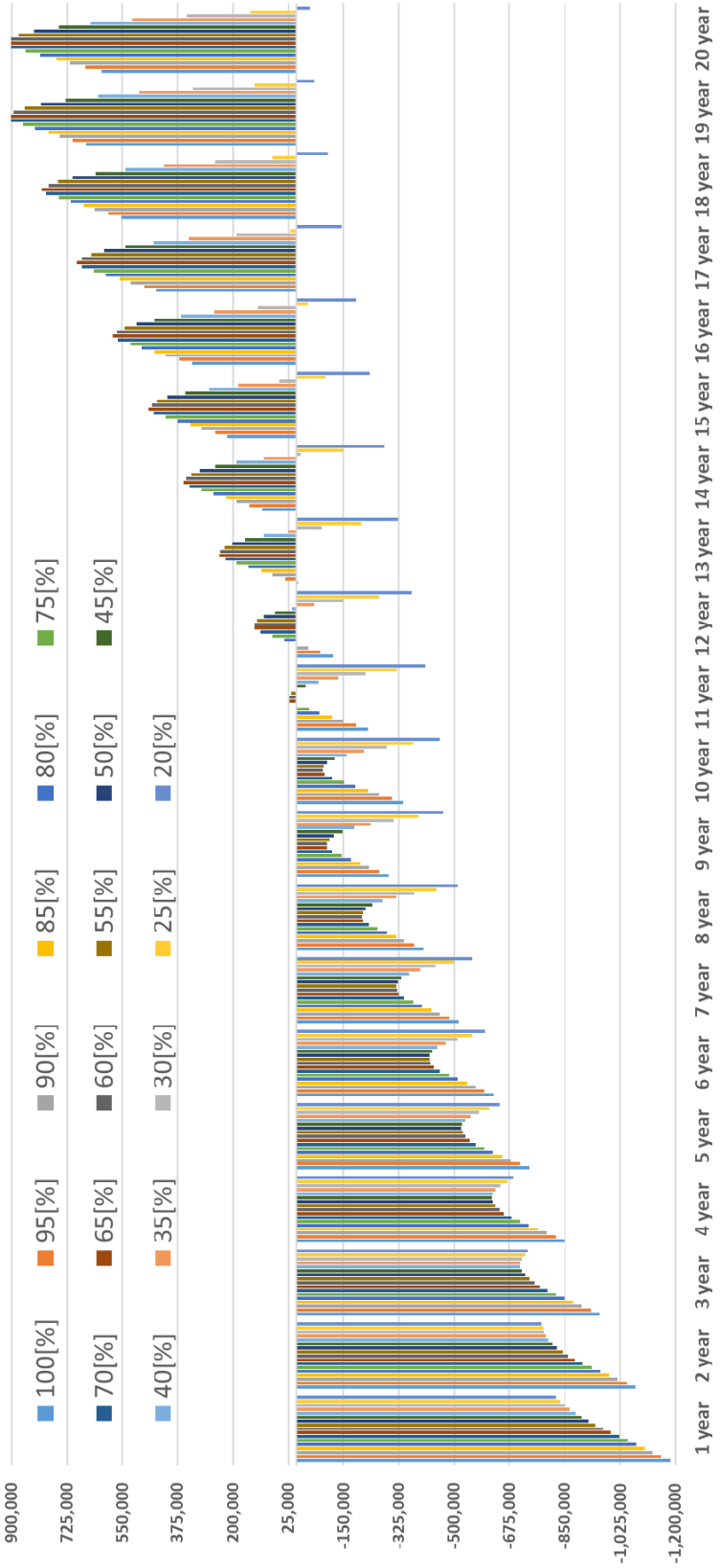

FIGURE 28. Detailed cash flow chart for different SI/PV ratios over 20 years.

This work is important for energy companies, policy makers and PV owners, to understand the limitations imposed, benefits of having SI capabilities and optimum sizing of PV panels, and SIs. The location of a household plays a large role in the maximum allowable energy export, and this should be taken into account in planning and operation.

APPENDIX

See Fig. 28.

ACKNOWLEDGMENT

The authors would like to thank K. Otani, T. Goda and J. Hashimoto for fruitful discussions.

REFERENCES

[1] *REthinking Energy 2017: Accelerating the Global Energy Transformation*, Int. Renew. Energy Agency, Abu Dhabi, UAE, 2017.
[2] J. P. Murenzi and T. S. Ustun, "The case for microgrids in electrifying Sub-Saharan Africa," in *Proc. 6th Int. Renew. Energy Congr. (IREC)*, Sousse, Tunisia, 2015, pp. 1–6.
[3] P. Buchana and T. S. Ustun, "The role of microgrids & Renewable energy in addressing Sub-Saharan Africa's current and future energy needs," in *Proc. 6th Int. Renew. Energy Congr. (IREC)*, Sousse, Tunisia, 2015, pp. 1–6.
[4] International Electrotechnical Commission (IEC), Standard IEC/TR 61850-90-7, Feb. 2013, "Communication Networks and systems for Power Utility Automation, Part 90-7: Object Models for Power Converters in Distributed Energy Resources (DER) Systems."
[5] J. Hashimoto, T. S. Ustun, and K. Otani, "Smart inverter functionality testing for battery energy storage systems," *Smart Grid Renew. Energy*, vol. 8, no. 11, pp. 337–350, 2017, doi: 10.4236/sgre.2017.811022.
[6] T. S. Ustun and S. Mekhilef, "Design and implementation of static synchronous series compensator with a soft-switching H-bridge inverter with DSP-based synchronization control," *Int. Rev. Elect. Eng.*, vol. 5, no. 4, pp. 1347–1353, 2010.
[7] A. H. Hubble and T. S. Ustun, "Scaling renewable energy based microgrids in underserved communities: Latin America, South Asia, and Sub-Saharan Africa," in *Proc. IEEE PES PowerAfrica*, Livingstone, Zambia, Jul. 2016, pp. 134–138.
[8] T. S. Ustun, H. Konishi, J. Hashimoto, and K. Otani, "Hardware-in-the-loop simulation based testing of power conditioning systems," in *Proc. IEEE 1st Int. Conf. Ind. Electron. Sustain. Energy Syst. (IESES)*, Hamilton, New Zealand, Jan./Feb. 2018, pp. 546–551.
[9] T. M. Wanzeler, J. P. A. Vieira, P. Radatz, V. C. Souza, and D. C. Pinheiro, "Assessing the performance of smart inverter Volt-Watt and Volt-Var functions in distribution systems with high PV penetration," in *Proc. Simposio Brasileiro Sistemas Eletricos (SBSE)*, Niterói, Brazil, 2018, pp. 1–6.
[10] D. P. Andrea, D. N. L. Pio, and M. Santolo, "Super twisting sliding mode control of smart-inverters grid-connected for PV applications," in *Proc. IEEE 6th Int. Conf. Renew. Energy Res. Appl. (ICRERA)*, San Diego, CA, USA, Nov. 2017, pp. 793–796.
[11] M. S. Hossan, V. Westfallen, E. A. Paaso, M. Avendano, and S. Bahramirad, "Usage of smart inverter Q-V droop functionality for irradiance variation induced voltage fluctuation reduction considering system uncertainty," in *Proc. IEEE Power Energy Soc. Innov. Smart Grid Technol. Conf. (ISGT)*, Washington, DC, USA, Feb. 2018, pp. 1–5.
[12] A. M. Howlader, S. Sadoyama, L. R. Roose, and S. Sepasi, "Experimental analysis of active power control of the PV system using smart PV inverter for the smart grid system," in *Proc. IEEE 12th Int. Conf. Power Electron. Drive Syst. (PEDS)*, Honolulu, HI, USA, Dec. 2017, pp. 497–501.
[13] Z. K. Pecenak, J. Kleissl, and V. R. Disfani, "Smart inverter impacts on california distribution feeders with increasing PV penetration: A case study," in *Proc. IEEE Power Energy Soc. Gen. Meeting*, Chicago, IL, USA, Feb. 2017, pp. 1–5.
[14] V. T. Dao, H. Ishii, and Y. Hayashi, "Voltage and energy loss assessment for systems with smart inverter functions of rooftop solar," in *Proc. 14th Int. Conf. Electr. Eng./Electron., Comput., Telecommun. Inf. Technol. (ECTI-CON)*, Phuket, Thailand, Jun. 2017, pp. 159–162.
[15] T. S. Ustun and Y. Aoto, "Impact of power conditioning systems with advanced inverter capabilities on the distribution network," in *Proc. 53rd IEEE Int. Universities Power Eng. Conf.*, Glasgow, Scotland, Sep. 2018, pp. 1–6.
[16] M. J. Parajeles, J. Quirós-Tortós, and G. Valverde, "Assessing the performance of smart inverters in large-scale distribution networks with PV systems," in *Proc. IEEE PES Innov. Smart Grid Technol. Conf., Latin Amer. (ISGT Latin Amer.)*, Quito, Ecuador, Sep. 2017, pp. 1–6.
[17] Y. Liu, C.-Y. Huang, Y.-R. Chang, and Y.-D. Lee, "Voltage impact mitigation by smart inverter control for PV integration at distribution networks," in *Proc. IEEE Int. Conf. Appl. Syst. Invention (ICASI)*, Chiba, Japan, Apr. 2018, pp. 192–195.
[18] D. Montenegro, M. Bello, B. York, and J. Smith, "Utilising observability analysis to cluster smart inverters on secondary circuits for residential deployment," *CIRED Open Access J.*, vol. 2017, no. 1, pp. 2572–2575, Oct. 2017.
[19] M. Tamai, T. Komatsu, T. Mitani, T. Goda, J. Hashimoto, and K. Otani, "Design of a novel distribution system simulator," in *Proc. Annu. Conf. Nat. Inst. Elect. Eng. Jpn. (IEEJ)*, Toyama, Japan, Mar. 2017, pp. 156–162.
[20] Ministry of Energy. (Aug. 8, 2017). *Transportation and Industry, Present Status and Promotion Measures for the introduction of Renewable Energy in Japan*. [Online]. Available: https://bit.ly/2IG6m2B
[21] *Position Paper on Self Consumption of PV Electricity*, EPIA Policy Commun. Working Group, Jul. 2013.
[22] C. Trueblood *et al.*, "PV measures up for fleet duty: Data from a tennessee plant are used to illustrate metrics that characterize plant performance," *IEEE Power Energy Mag.*, vol. 11, no. 2, pp. 33–44, Mar./Apr. 2013.
[23] *Recent Trends in Solar PV Market and Issues*, Ministry Energy, Transport Ind., 2014.
[24] Renewable Energy Promotion Center. *Fukushima Prefecture*. Accessed Dec. 1, 2018. [Online]. Available: http://fukushima-pv-hojo.org
[25] *Procurement Prices for 2015 Fiscal Year*, Ministry Energy, Transport Ind., 2015.

TAHA SELIM USTUN (M'04) received the Ph.D. degree in electrical engineering from Victoria University, Melbourne, VIC, Australia. He was an Assistant Professor of electrical engineering with the School of Electrical and Computer Engineering, Carnegie Mellon University, Pittsburgh, PA, USA. He is currently a Researcher with the Fukushima Renewable Energy Institute, National Institute of Advanced Industrial Science and Technology. His current research interests include power systems protection, communication in power networks, distributed generation, microgrids, and smartgrids. He is a member of the IEEE 2004 and 2800 Working Groups and the IEC Renewable Energy Management Working Group 8. He is also a Reviewer of reputable journals and has taken active roles in organizing international conferences and chairing sessions. He has been invited to run specialist courses in Africa, India, and China. He delivered talks for the Qatar Foundation, the World Energy Council, the Waterloo Global Science Initiative, and the European Union Energy Initiative.

YUKI AOTO graduated from Tokyo Kasei Gakuin Tsukuba Women's University, in 2001. She has been a Programming Specialist with the Energy Network Team, Renewable Energy Research Center, Fukushima Renewable Energy Institute, National Institute of Advanced Industrial Science and Technology, since 2015.